

# We are IntechOpen, the world's leading publisher of Open Access books Built by scientists, for scientists

5,000

Open access books available

125,000

International authors and editors

140M

Downloads

Our authors are among the

154

Countries delivered to

TOP 1%

most cited scientists

12.2%

Contributors from top 500 universities



WEB OF SCIENCE™

Selection of our books indexed in the Book Citation Index  
in Web of Science™ Core Collection (BKCI)

Interested in publishing with us?  
Contact [book.department@intechopen.com](mailto:book.department@intechopen.com)

Numbers displayed above are based on latest data collected.  
For more information visit [www.intechopen.com](http://www.intechopen.com)



# Novel OTEC Cycle Using Efficiency Enhancer

*Hosaeng Lee, Seungtaek Lim, Jungin Yoon and Hyeonju Kim*

## Abstract

The ocean thermal energy conversion (OTEC) plant is designed to improve the efficiency of the existing plants. Various researches are being conducted to increase the plant's efficiency and output with the use of an enhancer, and studies for performance improvement are also in progress from the Kalina and Uehara cycles to ejector pump OTEC (EP-OTEC). Their performance can be improved by increasing the evaporation pressure using an unused heat source and reducing the heat consumption using a reheating system and a regenerator. In the case of EP-OTEC, an ejector is installed near the turbine-exit to reduce the pressure and therefore increase the power output. In simulations and experiments conducted in this study, EP-OTEC showed 38% efficiency improvement from the basic cycle, which is due to the power output volume increase. The optimum ratio was derived by adjusting the pressure ratio. The demonstration plant to be developed in the future is expected to be applied to the high-efficiency OTEC demonstration plant with improved performance, and new technologies will be continuously developed considering economics and commercial viability.

**Keywords:** enhancer, reheater, regenerator, ejector pump OTEC, motive pump

## 1. Introduction

Ocean thermal energy conversion (OTEC) processes run under a much lower temperature gradient than that of the conventional thermal engines. The actual efficiency of a heat engine driven by the typical temperature difference of 20C is much smaller than the theoretical maximum due to heat and friction losses in the OTEC system. As such, from this perspective, OTEC may appear as a viable alternative energy source only after its thermal efficiency is well improved. As surface seawater is used as a heat source, which is essentially available in large quantities as an alternative energy source, many evaluators consider OTEC as one of the likely renewable energy-source candidates for large-scale power generation, especially in the tropical regions.

To improve the low-efficiency OTEC process, research has been focused on increasing their operational efficiency by using a high-quality heat source and using extra devices capable of improving the system's performance, in addition to locating and operating OTEC plants in tropical areas. In 1981, the Kalina cycle, named after its inventor, was reported as a new method for efficient thermal energy conversion to overcome some disadvantages of the well-known closed Rankine cycle. Whereas the Rankine cycle requires pure substances like ammonia, the Kalina cycle can use a mixture of ammonia and water [1, 2].

In 1994, the Uehara cycle was invented at Saga University to design and build a 4.5-kW power plant. The Uehara cycle includes a combined process of absorption and extraction, showing 1–2% better performance than that of the Kalina cycle. As shown in **Figure 1**, Bluerise in the Netherlands is conducting basic experiments on OTEC employing the Kalina cycle. As shown in **Figure 2**, a 4.5 kW-class experimental plant using the Uehara cycle was tested [3–6].

Recently, Amyra et al. developed a solar-collected OTEC (SC-OTEC) cycle of solar thermal energy. Their heat-collection system exchanges heat by utilizing surface water of a high temperature for evaporation and deep seawater of a low temperature for condensation to improve the power generation performance. In addition, Hakan Aydin suggested a performance change by increasing the superheating degree of the OTEC plant through the use of a solar collector [7, 8].

In 1982, Kyushu Electric (Japan) succeeded in constructing a 50-kW OTEC plant of a closed-loop cycle, utilizing waste heat from a diesel generator. In 2015, a 200-kW high-temperature power generation plant was built by KRISO (Korea),



**Figure 1.**  
*Experimental equipment of OTEC using the Kalina cycle (Bluerise).*



**Figure 2.**  
*4.5-kW experimental equipment of OTEC using the Uehara cycle (Saga Univ).*

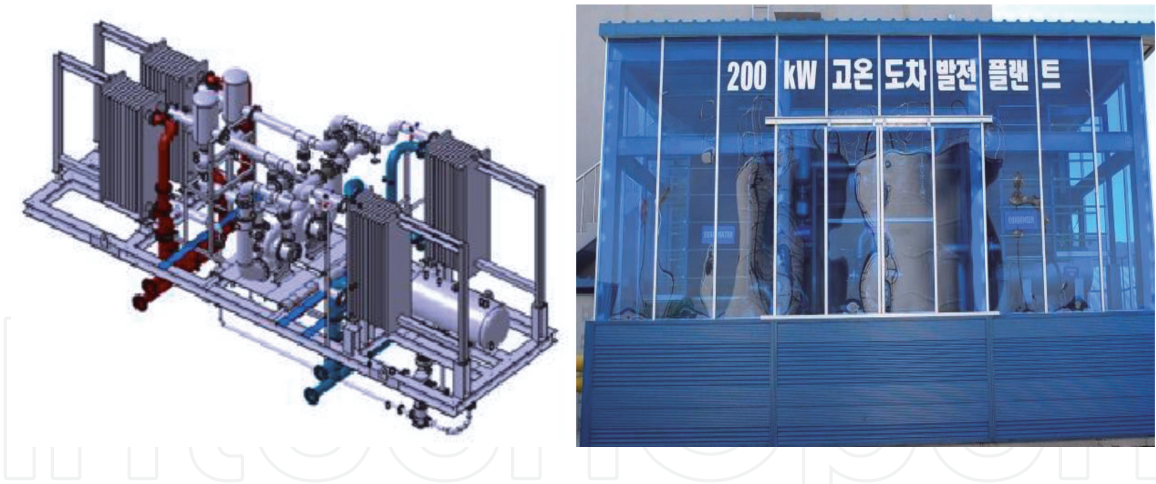


**Figure 3.** A 200-kW HOTEC plant using 80°C heat source (KRISO): 3D graphic (left) and photographic image (right).

which taps 70–80°C industrial waste heat and cold deep sea water, as shown in **Figure 3**. The plant improved the power generation efficiency by 7.8% through manufacturing components and a series of experiments, laying the foundation for the industrialization of the OTEC plant that taps external heat sources [9].

In addition to efficiency improvement, research has been carried out for heat reduction through the use of a reheating system and a regenerator. Recently, the power output and efficiency were additionally improved by Ejector and Pump-OTEC devised by Yoon et al., producing the maximum generation efficiency of 3.1% at the surface seawater temperature of 26°C [10].

## 2. Theory for OTEC cycle

OTEC plants generate electric power using the temperature difference between deep sea water and surface water. The system efficiency of OTEC can be expressed as the energy production rate of a turbine per thermal energy from evaporator. As the temperature of the heat source from the surface seawater increases, the vapor pressure of the seawater increases, the enthalpy increases from the inlet to the outlet of the turbine, and hence the process efficiency and power output are

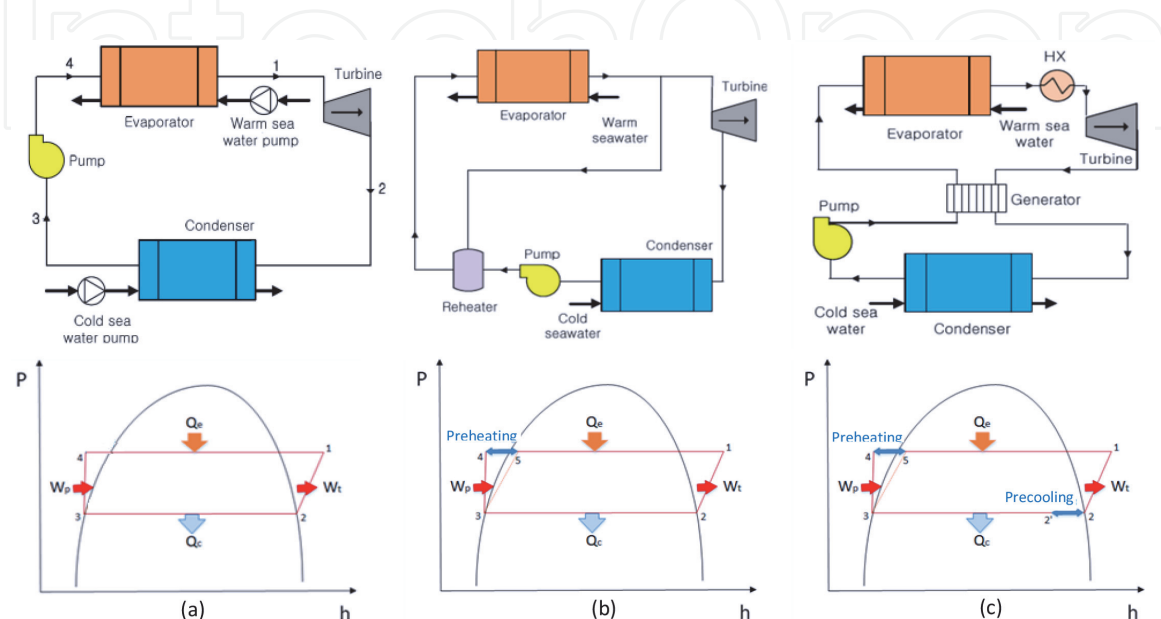


**Figure 4.** Schematic of basic and novel OTEC cycle: (a) basic cycle, (b) using reheater, (c) using regenerator.

enhanced. The use of high-temperature heat sources using collectors and heat storage tanks that can recover solar, geothermal, and industrial waste heat can further increase the process efficiency. On the other hand, one can increase the efficiency of the OTEC system by reducing the required amount of heat consumption in the evaporator. Toward this end, various studies have suggested methods to improve the efficiency of the closed OTEC cycle. One such way is by attaching a regenerator and a reheater.

The novel cycle that improves the efficiency of OTEC is transformed from the basic Organic Rankine Cycle. The basic ORC cycle repeats the process of reversible adiabatic compression of working fluid pump, constant pressure heat addition in evaporator, reversible adiabatic expansion in turbine, and constant pressure heat rejection in condenser. The OTEC using the basic Rankine cycle is shown in **Figure 4(a)** using the following balance equations:

$$Q_e = \dot{m}_r(h_1 - h_4) \quad (1)$$

$$W_t = \dot{m}_r(h_1 - h_2) \quad (2)$$

$$Q_c = \dot{m}_r(h_2 - h_3) \quad (3)$$

$$W_p = \dot{m}_r(h_3 - h_4) \quad (4)$$

where  $Q_e$  and  $W_t$  are the evaporation capacity and power output of turbine of the OTEC plant, respectively, and  $Q_c$  and  $W_p$  are the condenser capacity and the output of the working fluid pump, respectively.

On the other hand, in the case of the OTEC cycle with a reheater designed to reduce the evaporation capacity. The reheater improves the cycle efficiency by transferring heat to the working fluid flowing into the evaporator by recovering the heat of the superheated steam at the turbine outlet. The cycle is shown in **Figure 4(b)**. In the case of the method incorporating a regenerator, a part of the working fluid vaporized in the evaporator is bypassed, and the heat exchanged with the working fluid flows into the working fluid pump, as shown in **Figure 4(c)**. Then, the temperature of the working fluid flowing into the pump increases to reduce the evaporation capacity, thereby improving the cycle efficiency.

The equation for calculating the evaporation capacity with the regenerator or the reheater is changed to

$$Q_e = \dot{m}_{ww}(h_1 - h_5) \quad (5)$$

While on the one hand the cycle efficiency increases due to the reduced evaporation capacity, on the other hand, for the reheater case, the turbine output is represented as

$$W_t = (\dot{m}_r - \dot{m}_{rh})(h_1 - h_2) \quad (6)$$

because the mass flow rate of the working fluid flowing into the turbine is reduced by the amount supplied by the reheater. Here,  $\dot{m}_{rh}$  represents the mass flow rate of the working fluid flowing into the turbine.

### 3. Novel OTEC cycle using ejector

#### 3.1 Concept

To improve the performance of OTEC plants, research on efficiency improvement employing an ejector has been conducted. As mentioned earlier, the OTEC

system using an ejector pump is called “EP-OTEC.” As shown in the system schematic in **Figure 5** and the P-h diagram in **Figure 6**, some of the working fluid branched from the distributor installed at the inlet of the evaporator exchanges heat with the surface water of the ocean, which is a high heat source in the evaporator, and assumes a high-pressure gas state. This high-pressure working fluid drives the turbine and draws it into the suction section of the ejector through the pressure difference generated in the cycle. On the other hand, the remaining working fluid divided in the distributor is moved by the operating pump to the operating part of the ejector in the liquid state, without passing through the evaporator. At this time, the pressure rises according to the expected degree of lifting of the operating pump. This pressure rise is an important factor in the cycle because lower inlet pressure can be achieved when the actuator fluid is supplied with a stronger force to the nozzle of the liquid-vapor ejector. The lower inlet pressure in the OTEC system with ejectors leads to an increase in the pressure difference between the turbine inlet and outlet, which results in enhanced turbine performance. The operating fluid injected

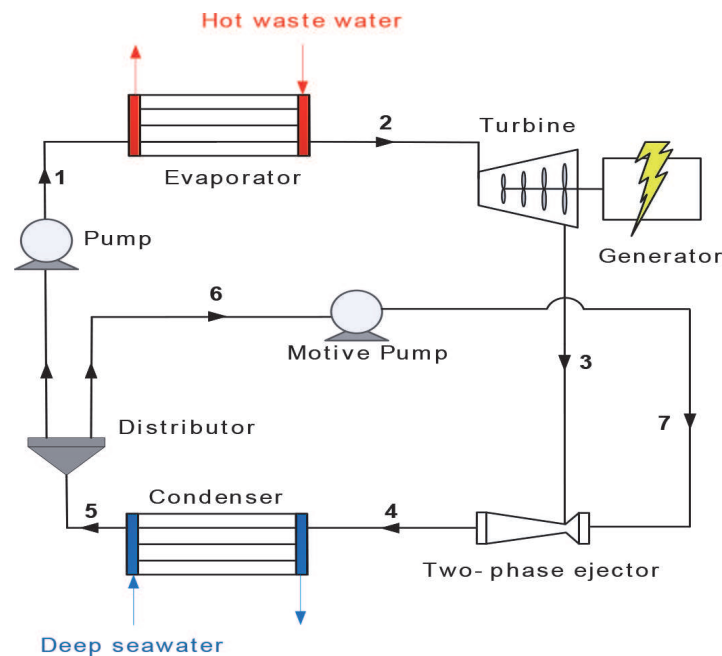


**Figure 5.**  
 Schematic of a two-phase ejector OTEC cycle.

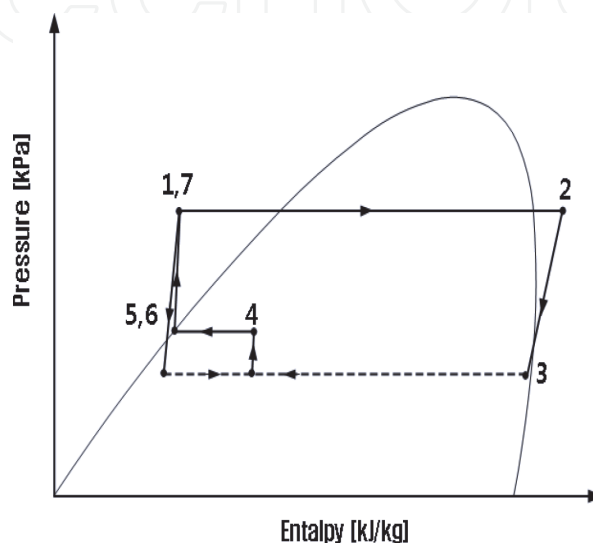


**Figure 6.**  
 P-h diagram of the EP-OTEC cycle.

from the ejector and the attracted suction fluid are mixed and discharged at the condensing pressure. The condenser condenses the working fluid after exchanging heat with deep water, which is a cooling source of the ocean. Finally, the working fluid is circulated by the pump, completing the full cycle.

The total power and net power of the turbine are determined by the mass flow through the turbine and the enthalpy change between the inlet and outlet of the turbine. Therefore, the enthalpy change due to the pressure change increased to generate more electricity using the turbine.

The power of the refrigerant pump is excluded from the turbine's total power equation (Eq. (7)), resulting in the turbine net power equation (Eq. (10)). A motive pump is newly applied to the current EP-OTEC system. The power input to the prime mover-pump is excluded from the turbine's total power because a high net power of the turbine is our goal as described using Eqs. (8) and (9). The system efficiency is expressed as the ratio between the input heat capacity and the output energy.

$$W_t = \dot{m}_r(h_2 - h_3) \quad (7)$$

$$W_{cp} = \dot{m}_r(h_1 - h_5) \quad (8)$$

$$W_{mp} = \dot{m}_r(h_7 - h_6) \quad (9)$$

$$W_{net} = W_t - W_{cp} - W_{mp} \quad (10)$$

**Figure 7(a)** is a schematic diagram of an ejector pump and heat exchanger ocean thermal energy conversion (EPX-OTEC) cycle with an ejector pump and an actuator evaporator. The basic power generation principle is the same as that of the existing Organic Rankine cycle (ORC), but some working fluid is branched at the condenser outlet (after the boosting pump) before passing through the heat exchanger, exchanging heat with the used heat source and (partially) vaporizing it into the working part of the ejector. At this time, some vaporized working fluid serves to smooth the traction of the fluid at the ejector intake, and increases the volume of the working gas (gaseous phase of the working fluid) drawn into the ejector. The efficiency of the system varies with the dryness, optimization focuses on phase transformation. In the EPX and DEPX cycles, the actuating heat exchanger introduces a heat source with a reduced temperature after evaporating the working fluid. A low-pressure atmosphere is formed at the suction part by the traction force of the working fluid introduced into the ejector operating part, thereby reducing the pressure at the turbine outlet and obtaining more power generation at the same flow rate than in the basic cycle. The remaining fluid—branched out of the condenser—exits the evaporator, driving the turbine and entering the ejector.

**Figure 7(b)** is a schematic diagram of the dual ejector pump and heat exchanger (DEPX)-ORC with a dual ejector pump and an actuator evaporator. The basic principle of DEPX is the same as that of EPX, but in DEPX-ORC, the working fluid splits into two branches after the operation of the actuating pump, and some of it passes through the actuating evaporator, as in the EPX cycle, and then enters the actuating part of the primary ejector and pulling the fluid out of the turbine.

The EPX and DEPX cycles have the same system analysis and calculation principles as the EP-OTEC cycle, and both cycles contain an additional heat source called “actuating evaporator.” Therefore, Eq. (11) expresses the amount of working fluid, branched by the P-h diagram and partial evaporation added by the amount

of enthalpy before and after working-part evaporation, as shown in **Figure 7(b)**. The said equation is based on the EPX cycle, and the additional heat source is calculated in the same way as in the DEPX cycle.

$$Q_{e.extra} = \dot{m}_{r.mot}(h_7 - h_6) \quad (11)$$

Accordingly, the efficiency of the entire cycle is also changed such as,

$$n = \frac{W_{net}}{Q_e + Q_{e.extra}} \quad (12)$$

As shown in **Figure 7(c)**, the efficiency can be maximized through cascade OTEC, which uses a condenser and an evaporator on the high- and low-temperature sides, respectively. When a refrigerant with different pressures is used in the high-/low-pressure part, low-/high-pressure refrigerant is formed in the high-/low-temperature part, and a low-/high-pressure load is formed in the high-/low-pressure part. Therefore, the high- and low-temperature sides were configured as DEPX-OTEC and EP-OTEC, respectively. Because it is difficult to apply the cascade

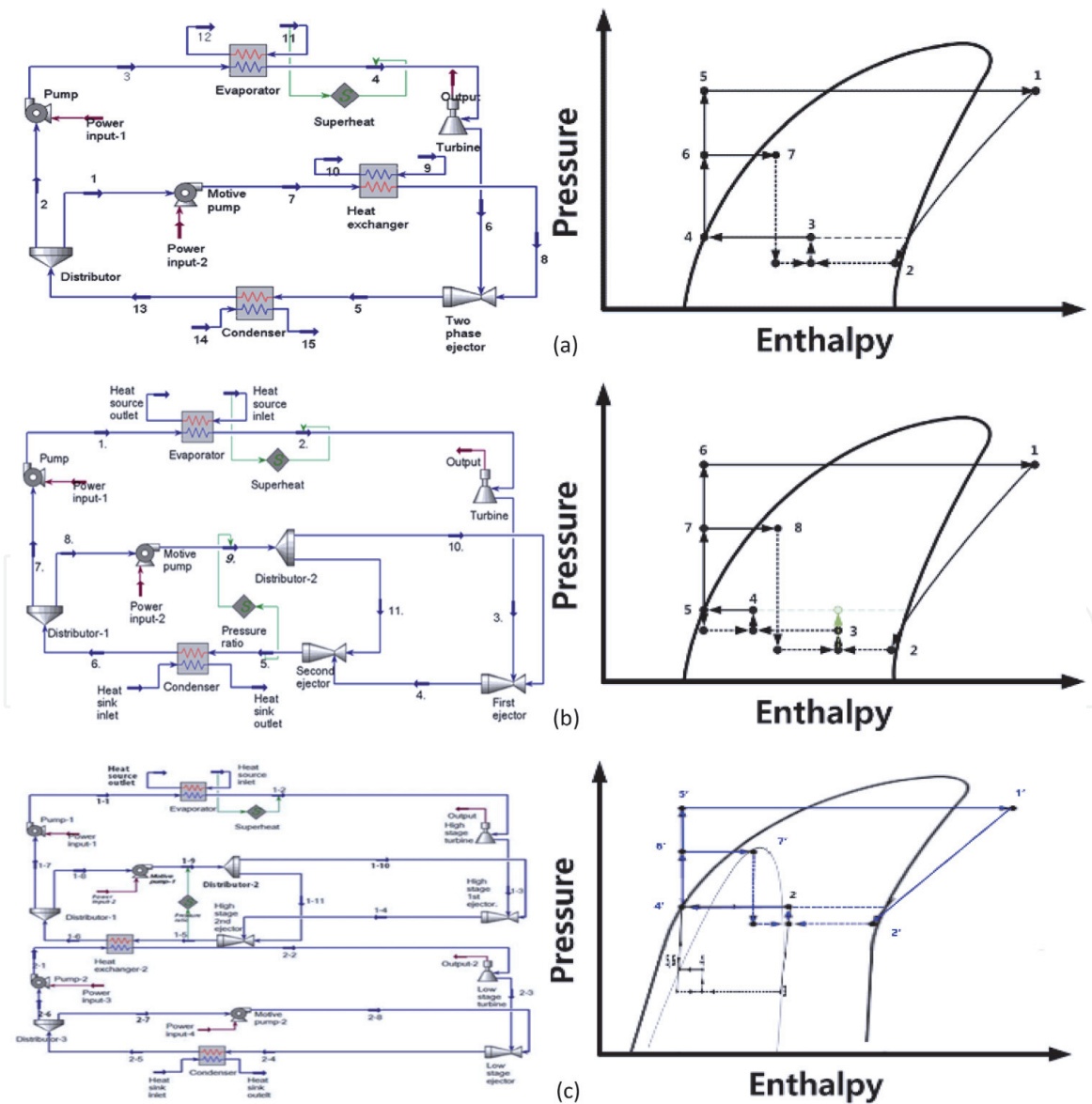


**Figure 7.** Schematic of novel OTEC cycle using ejector: (a) EPX, (b) DEPX-ORC, (c) cascade DEP.



method to the existing OTEC cycles using low-temperature heat sources, the cascade method is suitable to employ unused heat sources for medium and low OTEC systems.

### 3.2 Simulation results

**Table 1** shows the simulation conditions for the EP-OTEC system. The temperature of the marine surface water, which is a high heat source, was set to a typical temperature of the equator region of 29.0°C, which is almost invariant throughout the year. Deep seawater was applied to the condenser as the coolant, with the temperature kept about 5.0°C throughout the year.

The performances of conventional ocean thermal energy conversion and EP-OTEC were compared as the seawater temperature increased in the system with the

Parameters	Value
Surface seawater inlet temperature (°C)	24.0–29.0
Deep seawater inlet temperature (°C)	5.0
Temperature increase along the deep seawater intake pipe (°C)	5.8
Temperature increase along the surface seawater intake pipe (°C)	3.0
Pump efficiency (%)	65.0
Turbine efficiency (%)	80.0
Pressure ratio of motive and discharge of ejector (–)	3.0
Pressure drop at heat exchangers [kPa]	10.0

**Table 1.**  
*Analysis conditions.*

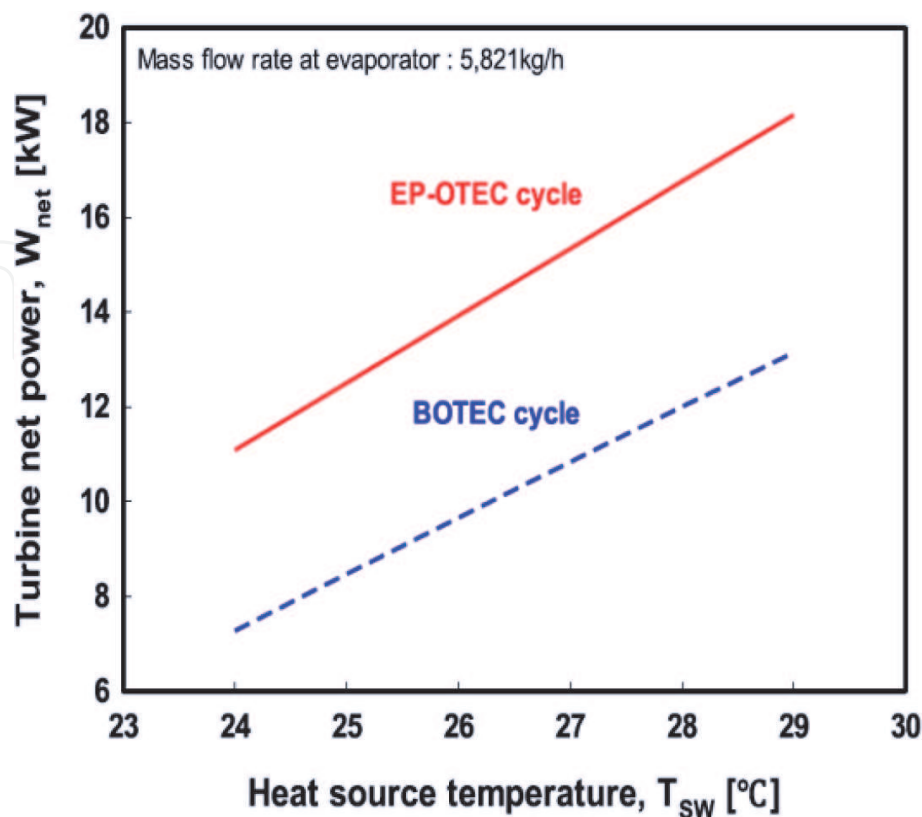


**Figure 8.**  
*Turbine net power with respect to the heat source temperature.*

R152a refrigerant when the ejector operating fluid mass was kept constant [11]. **Figure 8** shows the net turbine output of the EP-OTEC cycle as the surface seawater temperature varied from 24.0 to 29.0°C. As the higher temperature, heat source entered the evaporator, evaporator pressure increases, resulting in an increase in

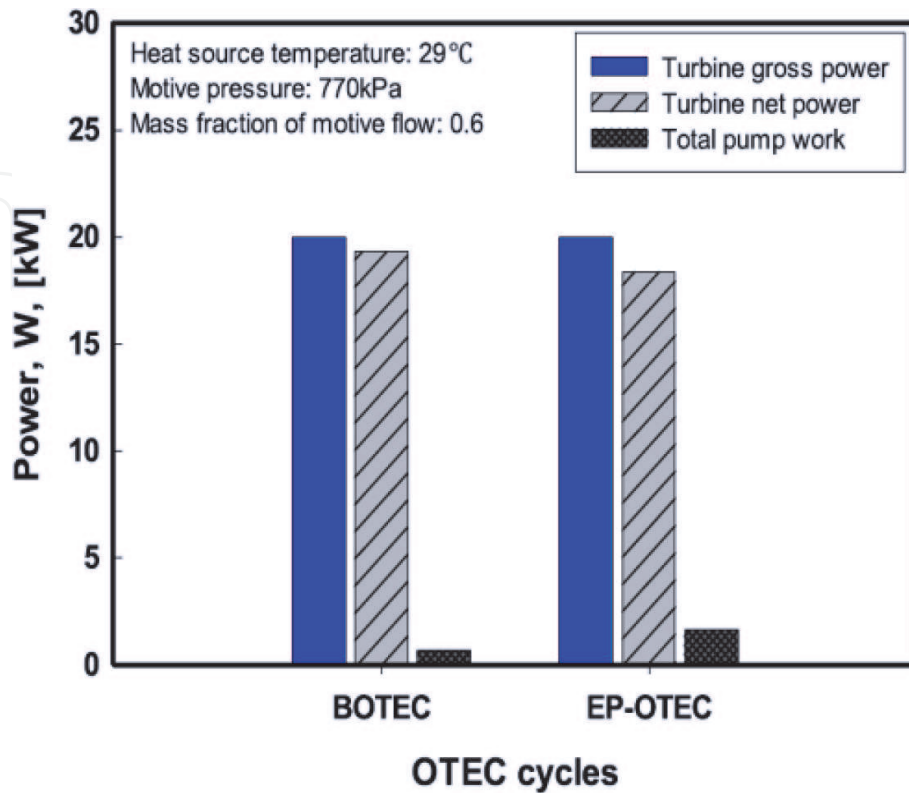


**Figure 9.**  
 Comparison of the turbine net power and the total pump work of the BOTEC cycle and the EP-OTEC cycle.

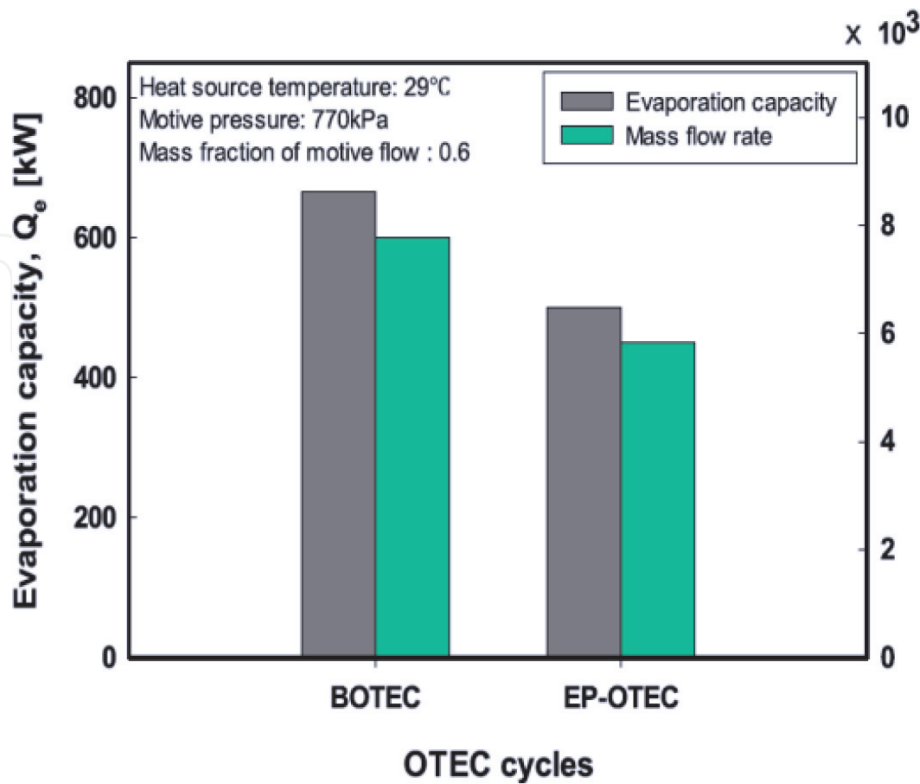


**Figure 10.**  
 Comparison of the evaporation capacity and the mass flow rate of the BOTEC cycle and the EP-OTEC cycle at the evaporator.

enthalpy from the inlet to the outlet of the turbine. For this reason, the turbine net power tended to increase with the surface seawater temperature at a constant mass flow rate to the evaporator. The utilization of the ejector and the motive pump lowered the turbine outlet pressure, and increased the enthalpy change of BOTEC and resulted in increased turbine power.

**Figures 9 and 10** show that the net turbine output of the EP-OTEC cycle is lower than that of the BOTEC cycle, in spite of the advantages described above. This was due to the amount of mass flow used as the synchronous fluid of the ejector in the EP-OTEC cycle. About 40% of mass entering the evaporator becomes the suction fluid later in the process and the remainder is used as the motive fluid without even entering the evaporator. As a result, the evaporation capacity of the EP-OTEC cycle is about 33% lower than that of the BOTEC cycle at the same total turbine output.

**Figure 11** compares the system efficiency of the EP-OTEC cycle with that of the BOTEC cycle for the 29°C surface seawater temperature and optimum conditions. The EP-OTEC cycle showed about 38% higher system efficiency than that of the BOTEC cycle, which confirms the superiority of the EP-OTEC to BOTEC.

In addition, comparative simulations of various cycles using ejectors were performed, employing unutilized heat sources like industrial waste heat. We designed an ORC engine using about 70–75°C temperature difference. In the heat exchanger of the ORC, the heat is exchanged with deep seawater heat sink and the low-temperature heat source below 80°C. Through the simulation, we compared the power generation and efficiency levels of EP, DEPX, and the cascade methods.

**Figure 12** shows a graph comparing the efficiency of the BOTEC used in this study and those of the EPX and DEPX cycles. The EPX cycle and DEPX-ORC showed the reflected efficiency level when a flow rate ratio of 1.0 outside the pressure recovery rate of 1.4 was applied. Under the same heat source, heat sink, and power generation conditions, EPX-ORC showed 10.06 and 5% higher efficiency than those of those of the BOTEC when basic ORC exhibited 9.58% efficiency. In the case, using DEPX that is 11.07% efficiency, about 15% higher than that of the basic cycle, was achieved.

In the cascade cycle, R245fa and R152a with low saturation pressure were applied at the higher and lower stages, respectively. The difference between the

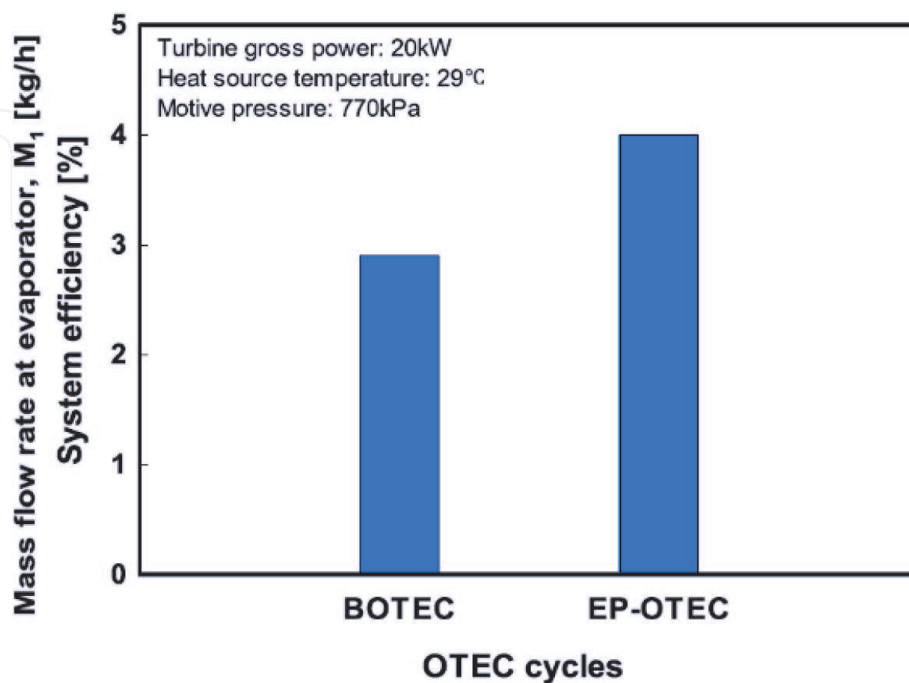


**Figure 11.**  
Comparison of the system efficiency between BOTEC and EP-OTEC cycle.

evaporation and condensation pressures of R152a at 75°C warm water and 5°C cold water requires a high pump head about 1500 kPa, suggesting that R152a has a larger turbine inlet/outlet pressure difference than R245fa and R600a under the same temperature conditions. The cascade cycle was developed to enable secondary power production at a small temperature difference through its application at the

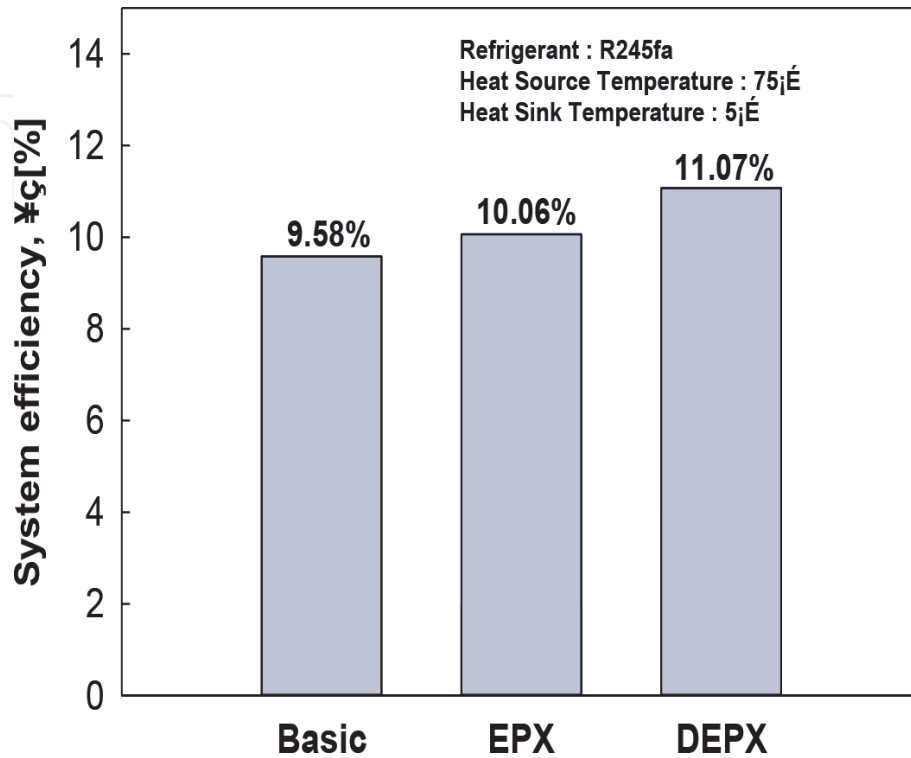


Figure 12.  
 System efficiency comparison with basic cycle between EPX and DEPX cycles.

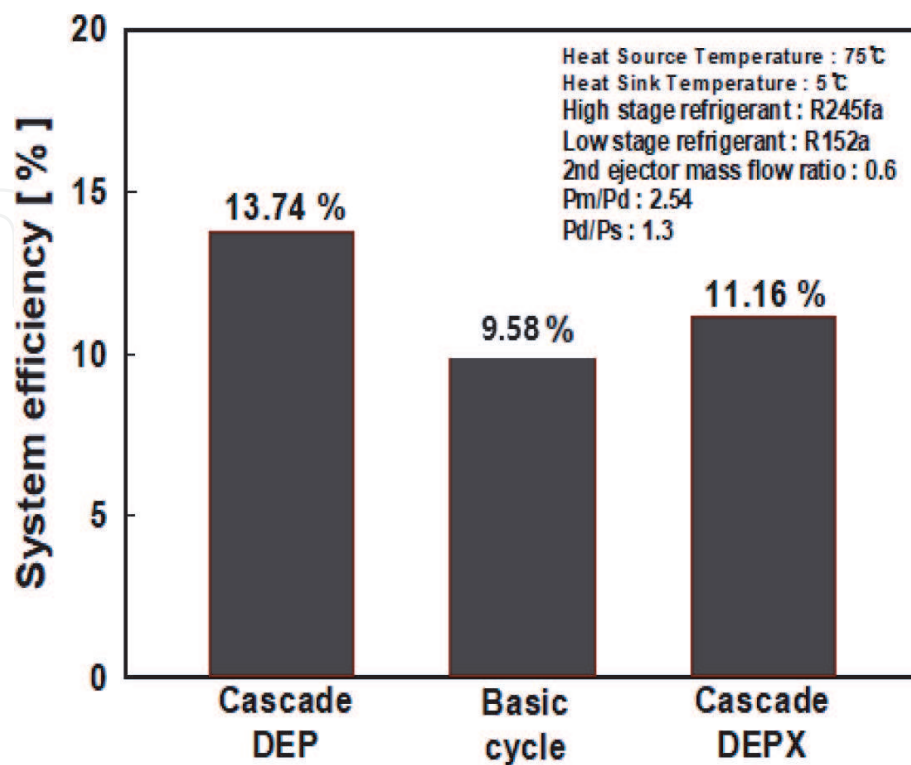


Figure 13.  
 System efficiency comparison with basic cycle between cascade DEP and cascade DEPX cycles.

lower stage of the cascade system. At the high stage, the DEP and DEPX cycles are applied to improve the system performance. **Figure 13** shows the improved efficiency of the cascade DEP and DEPX cycles over the BOTEC. The high-stage secondary ejector was fixed at a mass flow ratio of 0.6, and the ejector pressure recovery rate was 1.3. The simulation results show that the system efficiency of the cascade DEP and DEPX cycles improved by 43.3 and 16.5%, respectively, over the BOTEC.

### 3.3 Experiment results

An experimental study was conducted to verify the performance of the ejector under various operating conditions. The operating pressure, discharge pressure, and flow rate were set as the experiment variables as they determine the ejector performance.

**Figures 14 and 15** show the device diagram of the ejector performance tester and the actual test device, respectively. The refrigerant side of the experiment apparatus consists of three heat exchangers, a refrigerant pump, two flow meters, an ejector, and flow-control valves. The temperature condition of the operating fluid is achieved by heat exchanging process with the hot water heated by the electric heater at the operating-side heat exchanger (Motive HX), while the pressure is controlled by the refrigerant-side Pump1. The suction fluid is transferred by the ejector traction force from the receiver behind the condenser, and is then vaporized through heat exchanging process with the hot fluid in the heat exchanger (HX). The working fluid discharged from the ejecting part of the ejector in the mixed liquid-gas state passes through the condenser before being condensed into liquid state through heat exchange with low-temperature brine. The mass flow rate of each fluid was adjusted using the installed valves and measured using flow meters

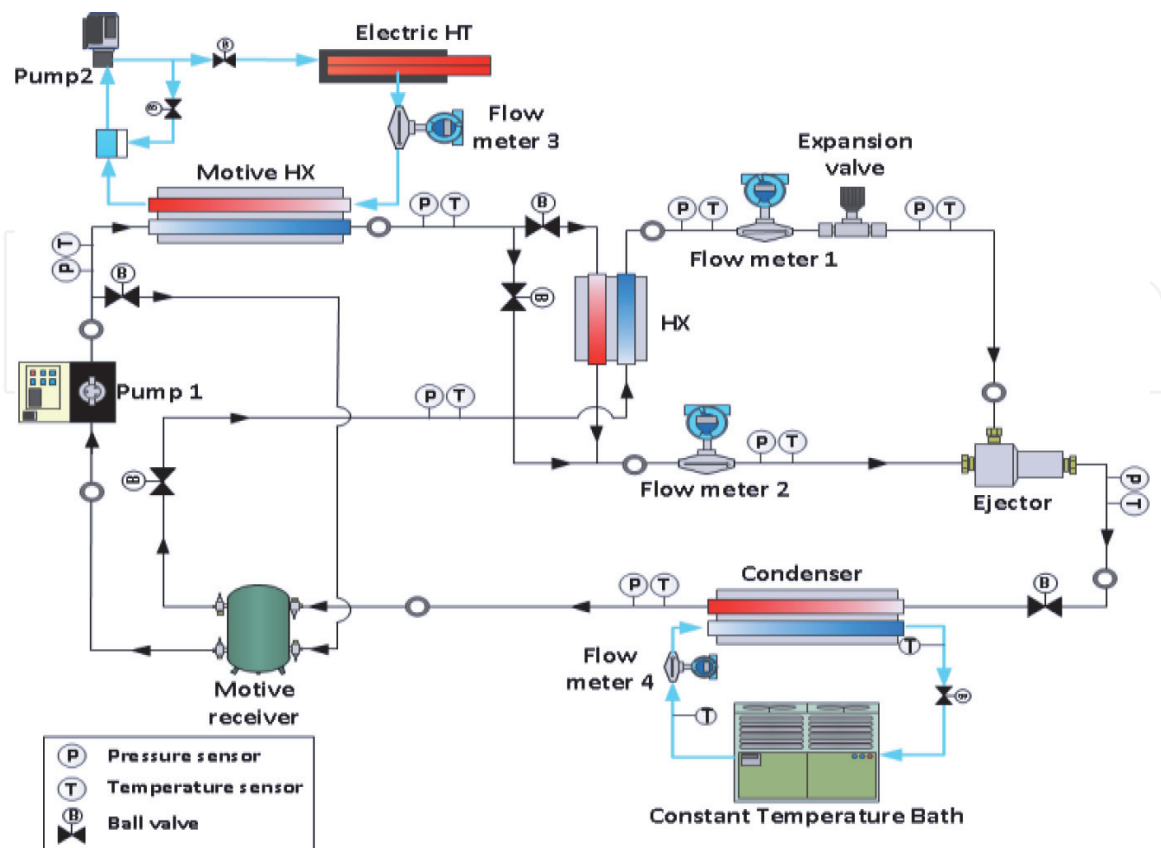


**Figure 14.**  
*Schematics of ejector performance experiment.*

installed in the operation and suction parts. The basic experiments for ejector performance verification involves

1. design and manufacture of laboratory-scale ejector basic preliminary test equipment

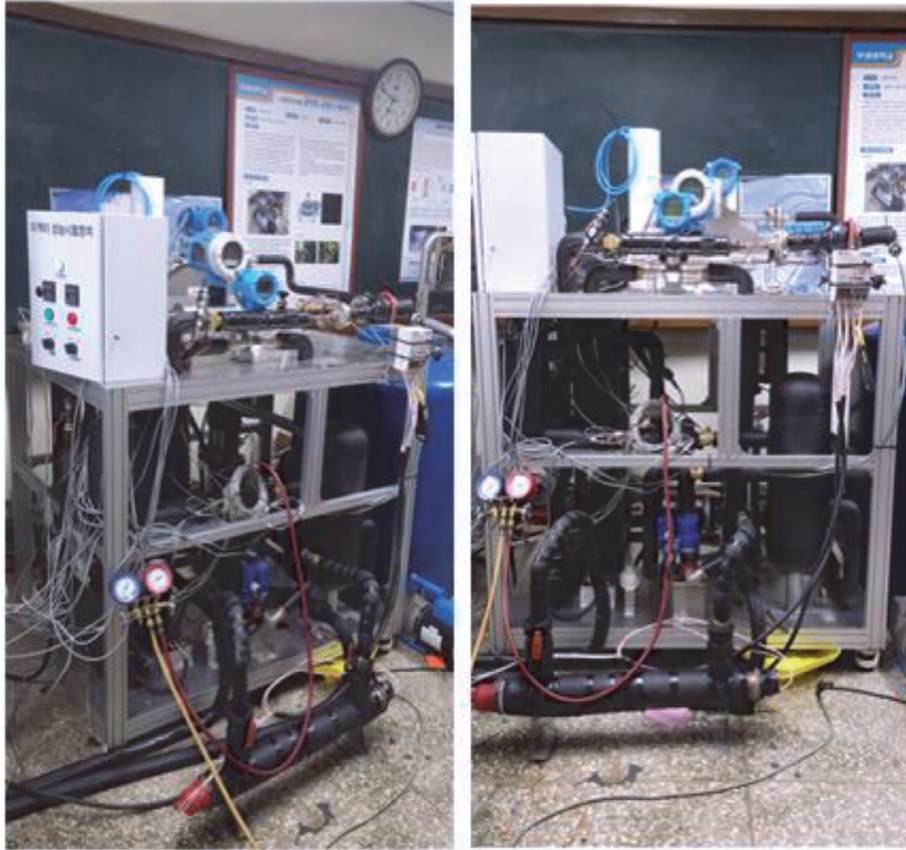


**Figure 15.**  
*Experimental apparatus of ejector performance.*

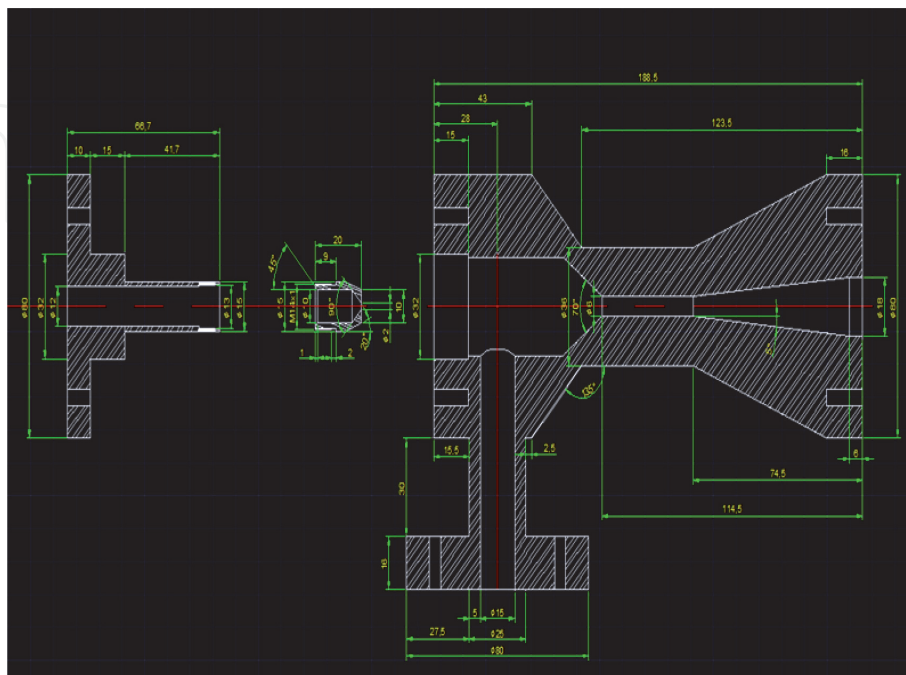


**Figure 16.**  
*Design drawing of ejector.*

2. performance verification of the ejector according to the working pressure, discharge pressure, and flow rate ratio
3. supply of hot water through the electric heater of the high-temperature part, a heat source, and heat needle supply through a low-temperature thermostat connected to the low-temperature part



Figure 17.  
Manufactured ejector (body).

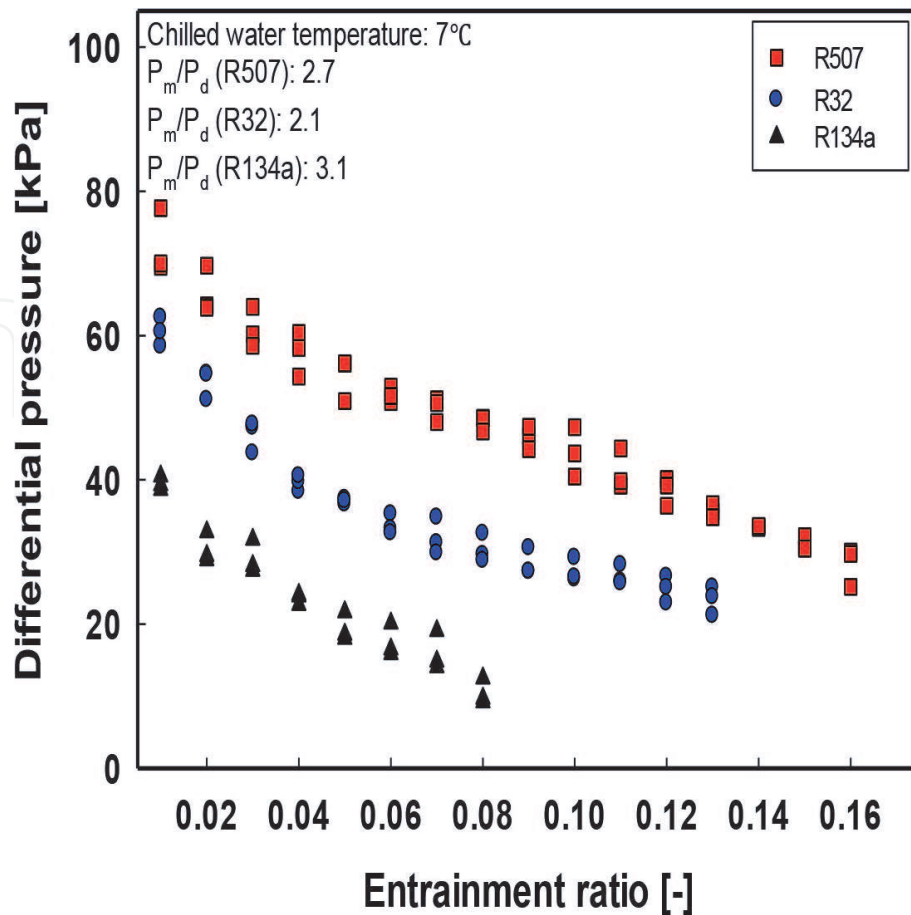
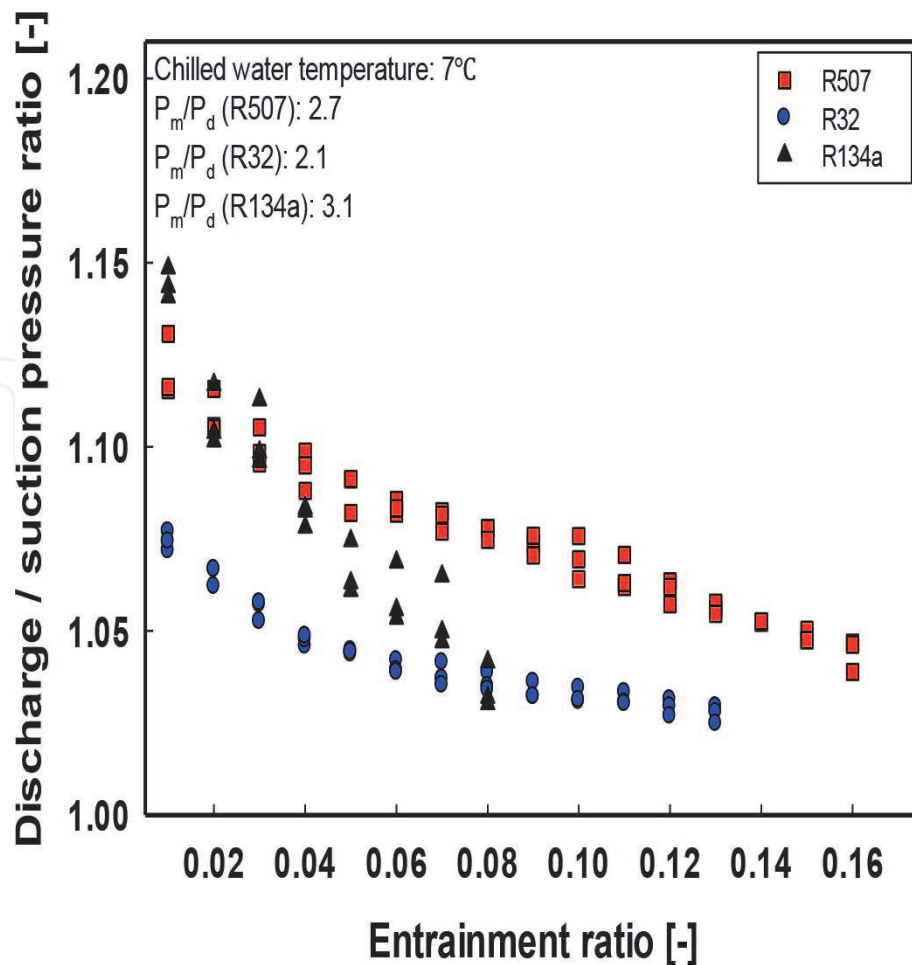


Figure 18.  
Differential pressure with respect to entrainment ratio.



**Figure 19.**  
 Discharge/suction pressure with respect to entrainment ratio.

4. selection of working fluid for the refrigeration-combined temperature generator system considering the gas density and efficiency
5. working fluids of R32, R507, and R134a, which have relatively high gas densities, applied as the working fluid at the beginning of the experiment

An ejector was fabricated for the demonstration experiment of the proposed OTEC system, with its specifications and completed product shown in **Figures 16** and **17**, respectively.

**Figure 18** shows the difference between the discharge and suction pressures according to the flow rate ratio of the ejector. All the three applied fluids showed a tendency to decrease the pressure difference as the flow rate ratio increased. This was the drop in pressure that occurred as the flow rate below the traction force of the ejector was supplied, and the quantitative level of the pressure difference was different for each working fluid. As R507 has the smallest specific volume among the three working fluids, R507 has the largest pressure difference under the condition that a certain mass flow rate is drawn into the ejector. R32 is a refrigerant with a gas density about 46% less than that of R507 having the gas density of  $3.43 \text{ g/cm}^3$ , but also with a relatively small pressure differential due to the limited lift of the pump. R134a was the smallest-gas-density refrigerant among the three working fluids, and therefore providing the smallest pressure difference.

**Figure 19** shows the ratio of the discharge and suction pressures according to the flow rate ratio of the ejector. This ratio indicates the pressure recovery performance of the ejector. The pressure recovery rate is calculated based on the discharge-unit pressure and the pressure difference between the discharge and suction sides.



On the other hand, the pressure recovery rate of R32 was slightly lower due to its smaller pressure difference and higher discharge pressure, compared to R507.

The experimental study that was conducted using the flow rate ratio of the ejector for the OTEC system is summed up below. As the flow rate ratio of the ejector increased, the pressure difference between the discharge and suction parts decreased, and the level of differential pressure varied with applied refrigerants. As the refrigerant R507 had the smallest specific volume among the three refrigerants that were used, the highest differential pressure was generated in all its flow rate ratio sections. On the other hand, the R134a refrigerant was found to exhibit high-pressure recovery performance ( $P_d/P_s$ ) although differential pressure is relatively small due to its low discharge pressure.

#### **4. Further plan**

Korea Research Institute of Ships and Ocean Engineering aims to complete the OTEC plant at Kiribati by 2021 (**Figure 20**). The production and testing of 1 MW-class OTEC plant such as a 20-kW pilot plant is in progress. After the completion of the domestic demonstration in 2019, onsite construction will be conducted for 2 years. Considering the initial investment cost and the system safety, a closed-temperature generator using R32 refrigerant was decided to be applied. As the current project is to establish a demonstration plant for the first commercial OTEC plant, it will be necessary to apply a high-efficiency system considering economic aspect and performance improvement. The reheating and regeneration cycles mentioned above and the EP-OTEC cycle with ejectors are considered to be competitive in terms of high performance and cost-effectiveness, compared to the conventional Kalina or Uehara cycles.

The following questions should be answered with regard to the future commercialization of the improved OTEC plant:



**Figure 20.**  
*3D design of 1-MW OTEC plant in Kiribati (KRISO).*

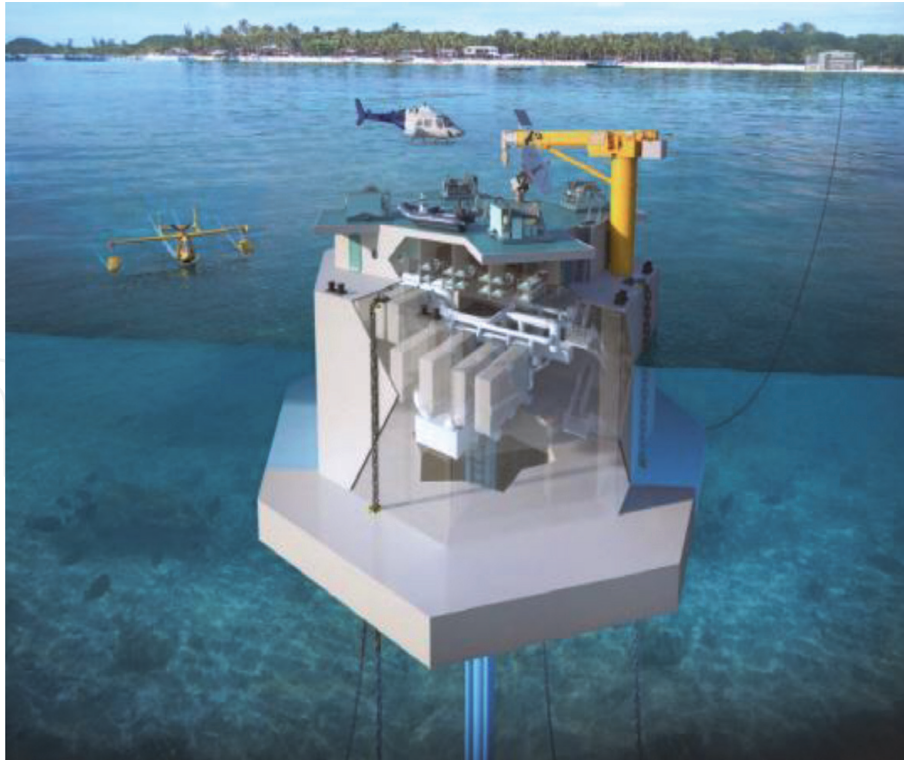


**Figure 21.**  
*3D design of advanced future OTEC plant (KRISO).*

1. Is the output or efficiency of the improved OTEC plant system excellent enough to be commercialized?
2. Is the application of the improved OTEC system economically competitive?
3. How long does it take to return the initial investment after the first day of operation?
4. Is the improved OTEC system environmentally friendly and safe to operate?
5. Are operations of the improved OTEC system straightforward for educated operators?
6. Can the improved OTEC system be easily automatized and be under the unmanned operation?

Through the study of improved OTEC based on the above considerations, we expect that high-efficiency stabilized power plants, shown in **Figure 21**, become available in the near future, while the first commercializable OTEC will be running at Kiribati in a few years.

## **Acknowledgements**

This work was financially supported by the National R&D project of “Development of 1MW OTEC demonstration plant (4/6)” (PMS4080) funded by the Ministry of Oceans and Fisheries of the Republic of Korea.

IntechOpen

## **Author details**

Hosaeng Lee<sup>1\*</sup>, Seungtaek Lim<sup>1</sup>, Jungin Yoon<sup>2</sup> and Hyeonju Kim<sup>3</sup>

1 Seawater Energy Plant Research Center, Korea Research Institute of Ships and Ocean Engineering, Goseong-gun, South Korea


2 Department of Refrigeration and Air-Conditioning Engineering, College of Engineering, Pukyong National University, Busan, South Korea

3 Offshore Plant and Marine Energy Research Division, Korea Research Institute of Ships and Ocean Engineering, Daejeon, South Korea

\*Address all correspondence to: [hslee@kriso.re.kr](mailto:hslee@kriso.re.kr)

## **IntechOpen**

---

© 2020 The Author(s). Licensee IntechOpen. This chapter is distributed under the terms Commons Attribution - NonCommercial 4.0 License (<https://creativecommons.org/licenses/by-nc/4.0/>), which permits use, distribution and reproduction for non-commercial purposes, provided the original is properly cited. 

## References

- [1] Avery WH, Wu C. Renewable Energy from the Ocean: A Guide to OTEC. England: Oxford University Press; 1994
- [2] Galbraith K. Generating Energy from the Deep. The New York Times; 29 Apr 2009
- [3] Uehara H, Nakaoka T. Development and Prospective of Ocean Thermal Energy Conversion and Spray Flash Evaporator Desalination. Saga, Japan: Saga University; 2007
- [4] Finney AK. Ocean thermal energy conversion. Guelph Engineering Journal. 2008;(1):17-23
- [5] Salz K. An assessment of the performance and potential of OTEC innovation clusters worldwide [thesis]. Delft University of Technology; 2018
- [6] Uehara Cycle in Saga Univ [Internet]. Available from: [http://www.ioes.saga-u.ac.jp/en/facilities/ioes\\_facilities](http://www.ioes.saga-u.ac.jp/en/facilities/ioes_facilities)
- [7] Amyra MY, Othman N'a, Sarip S, Ikegami Y, Chik MAT, Othman N, et al. Simulation study on enhancing hydrogen production in an ocean thermal energy (OTEC) system utilizing a solar collector. Journal Teknologi (Sciences & Engineering). 2015;77(1): 23-31. DOI: 10.11113/jt.v77.4145
- [8] Aydin H. Performance analysis of a closed-cycle ocean thermal energy conversion system with solar preheating and superheating [thesis]. University of Rhode Island; 2013
- [9] Lee HS, Lim ST, Moon JH, Kim HJ. Performance assessment for high Temperature OTEC plant. Proceedings of Renew 2016, 2nd International Conference on Renewable Energies Offshore. 2016:475-480
- [10] Lee HS, Kim HJ, Jung DH, Moon DS. A study on the improvement for cycle efficiency of closed-type OTEC. Journal of the Korean Society of Marine Engineering. 2011;35(1):46-52. DOI: 10.5916/jkosme.2011.35.1.046
- [11] Yoon JI, Seol SH, Son CH, Jung SH, Kim YB, Lee HS, et al. Analysis of the high-efficiency EP-OTEC cycle using R152a. Renewable Energy. 2017;105: 366-373. DOI: 10.1016/j.renene.2016.12.019